

High proton conductivity in a charge carrier induced Ni(II)-metal-organic framework

Debabrata Chakraborty,^a Arijit Ghorai,^b Piyali Bhanja,^c Susanta Banerjee,^b Asim Bhaumik*^a

^a*School of Materials Sciences, Indian Association for the Cultivation of Science, 2A & 2B, Raja S.C. Mullick Road, Jadavpur, Kolkata-700032, India*

^b*Materials Science Centre, Indian Institute of Technology Kharagpur, Kharagpur 721302, India*

^c*Materials Chemistry Division, CSIR - Institute of Minerals & Materials Technology, Bhubaneswar, Odisha 751013, India*

Corresponding author: msab@iacs.res.in

Supporting Information

Entry	Table of contents	Page No
Experimental	¹ H-NMR, ¹³ C-NMR and ³¹ P NMR spectra (Figure S1-S7) of TPE, TPE-Br, TPE-Ester and TPE-Acid (H ₈ L ligand).	S2-S5
Figure S8	Solid state UV-Visible spectra of as-synthesized H ₈ L-Ni-MOF and H ₈ L-ligand.	S6
Figure S9	Direct optical band gap measurement of H ₈ L-Ni-MOF material using Tauc equation	S7
Figure S10	UHR-TEM images of H ₈ L-Ni-MOF material at different magnifications.	S8
Figure S11	HADDF images and elemental mapping of H ₈ L-Ni-MOF material containing elements C, P, O, and Ni atom.	S9
Figure S12	Full scale XPS survey spectrum of H ₈ L-Ni-MOF.	S10
Figure S13	Thermogravimetric plot of H ₈ L-Ni-MOF.	S11
Figure S14	Water uptake (weight %) of H ₈ L-Ni-MOF with time at 30 °C under 98% RH and PXRD pattern of the H ₈ L-Ni-MOF.	S12
Table S1.	Proton conductivity of H ⁺ @H ₈ L-Ni-MOF at 98% RH in different temperatures.	S13
Figure S15	PXRD data of as-synthesized, H ⁺ @H ₈ L-Ni-MOF and washed MOF	S14

Experimental Section

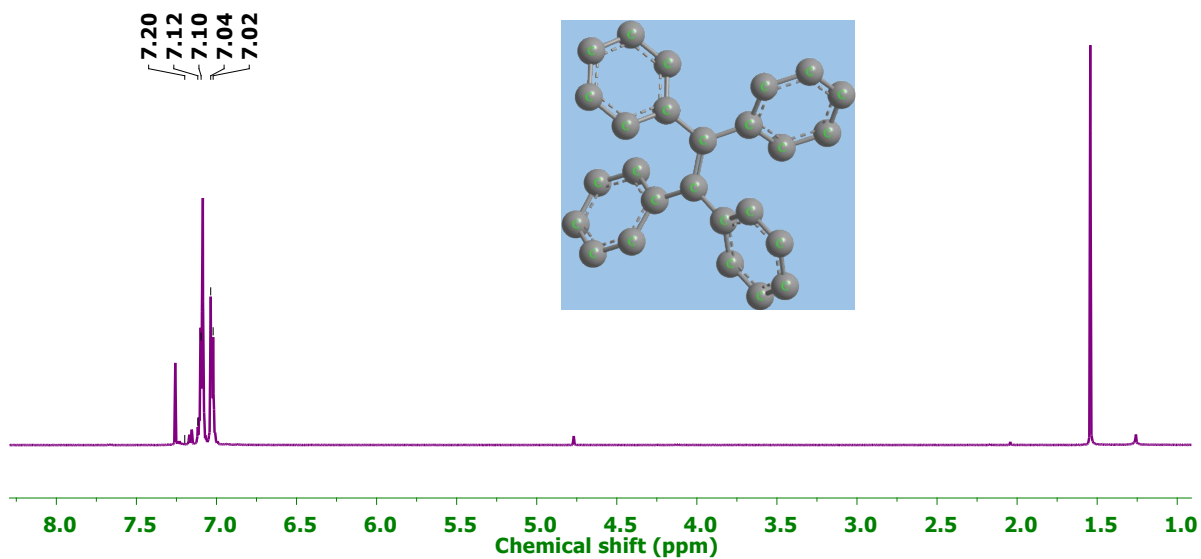


Fig.S1. ^1H NMR spectra of TPE.

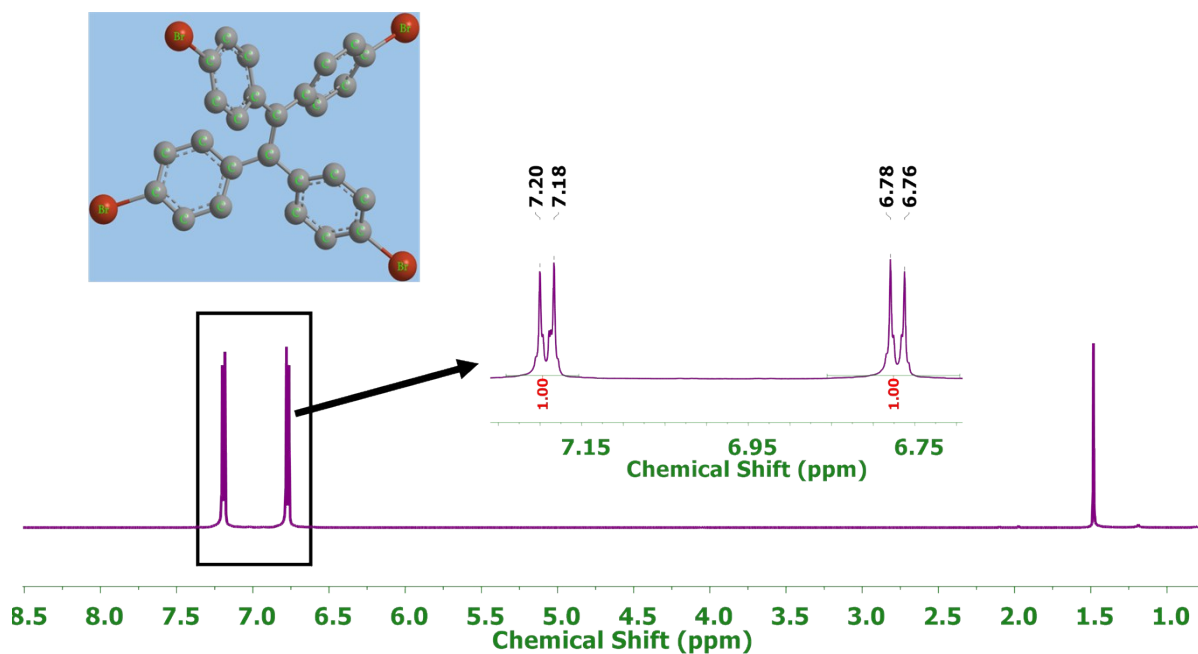


Fig. S2. ^1H NMR spectra of TPE-Br.

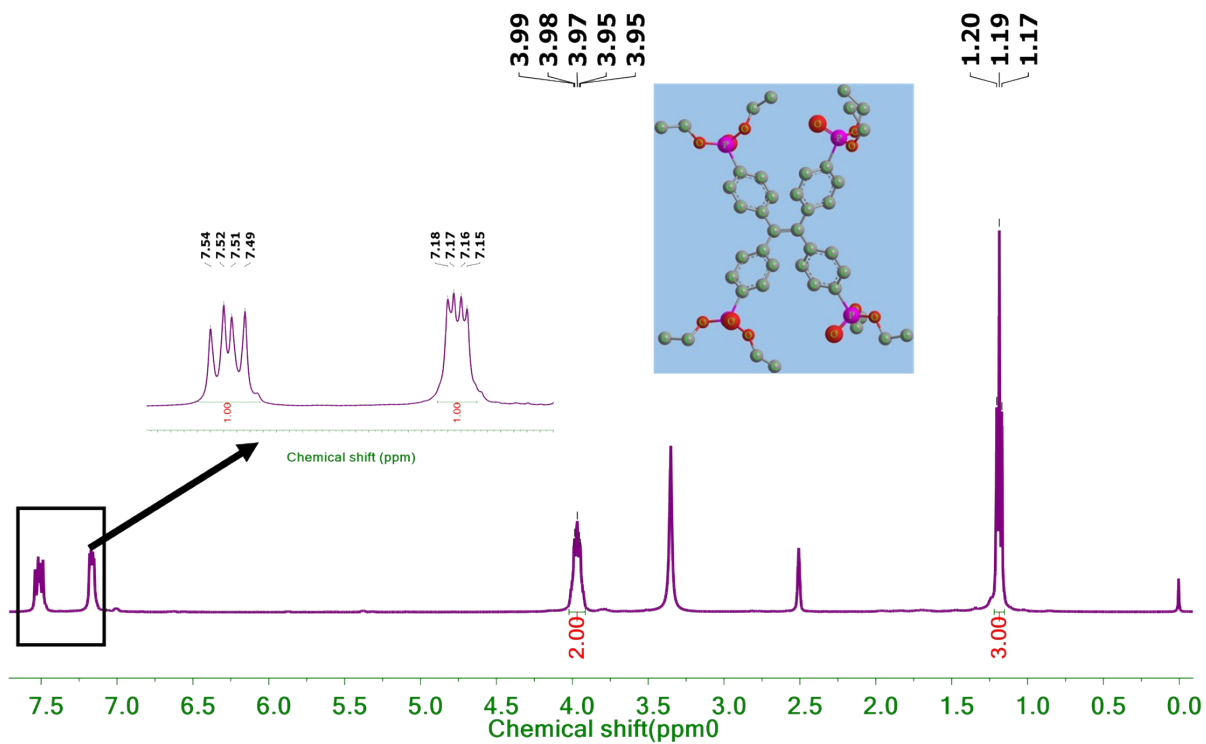


Fig. S3. ^1H NMR spectra of TPE-PE.

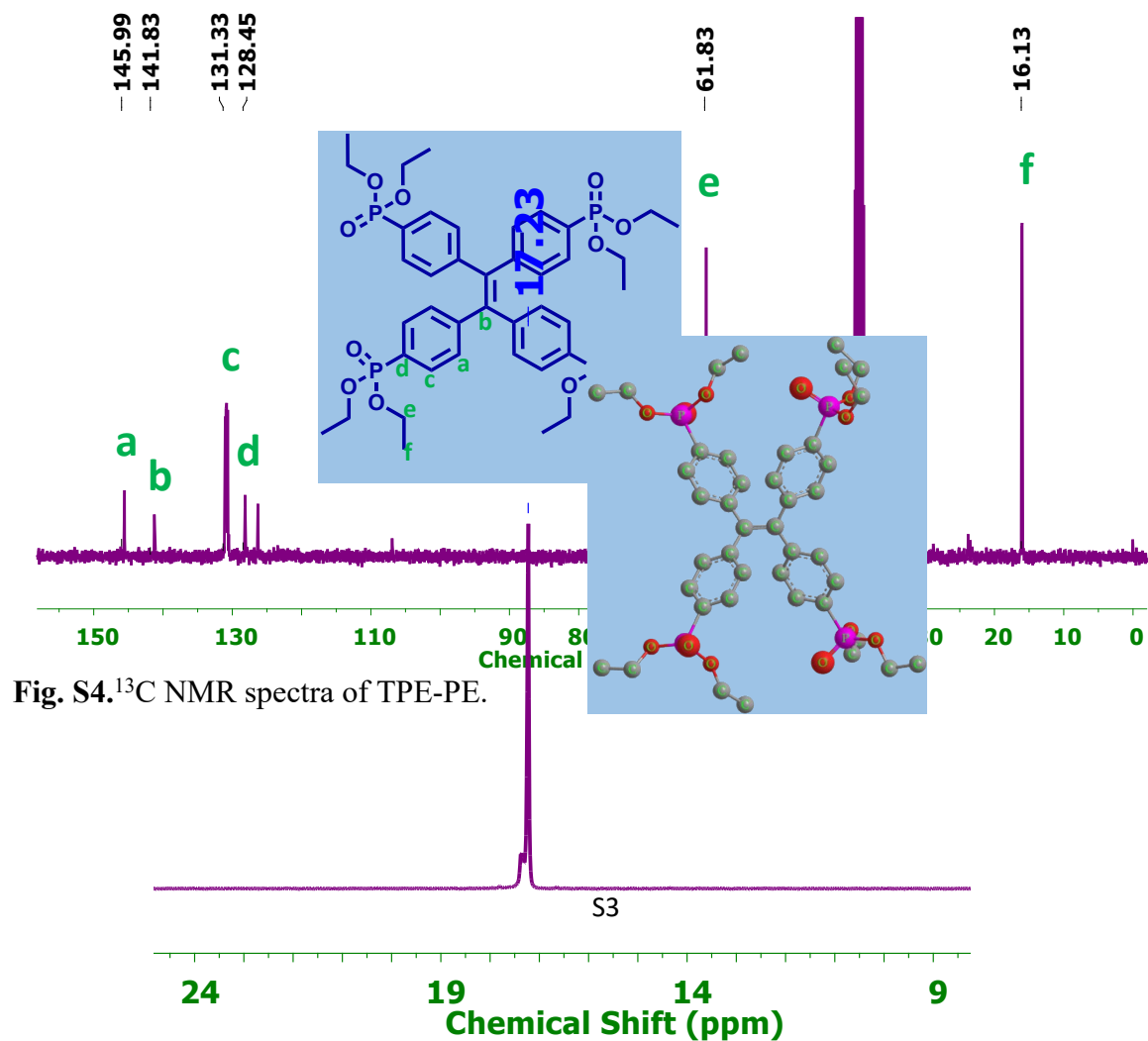


Fig. S4. ^{13}C NMR spectra of TPE-PE.

Fig. S5. ^{31}P NMR spectra of TPE-PE.

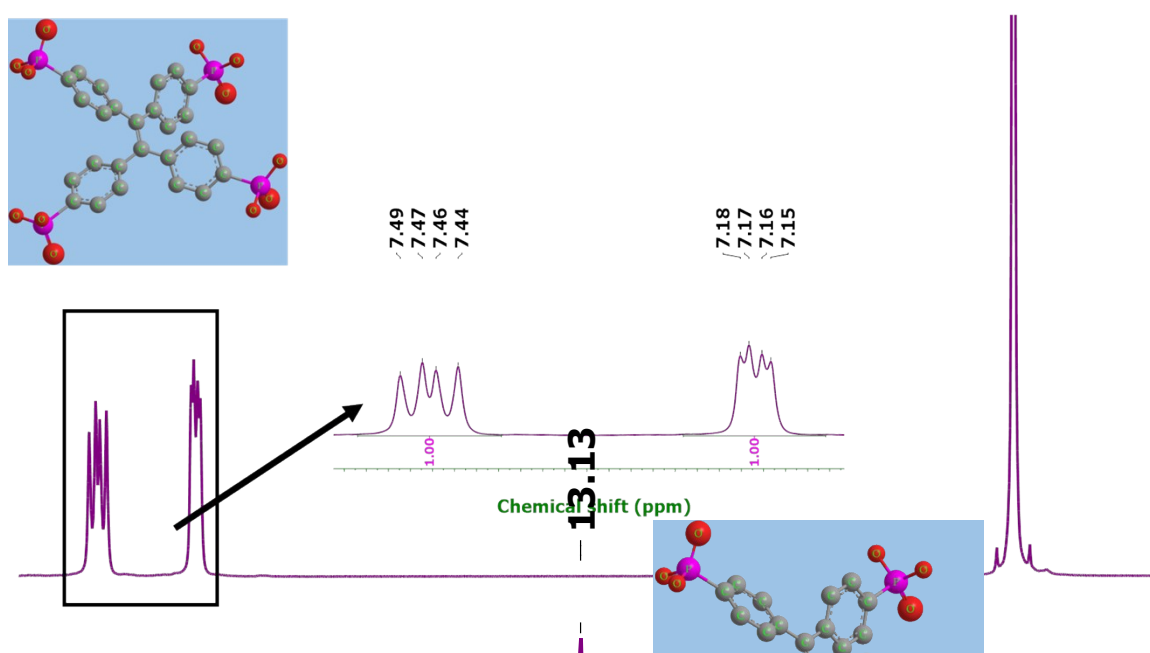


Fig. S6. ^1H NMR Spectra of TPE-PA.

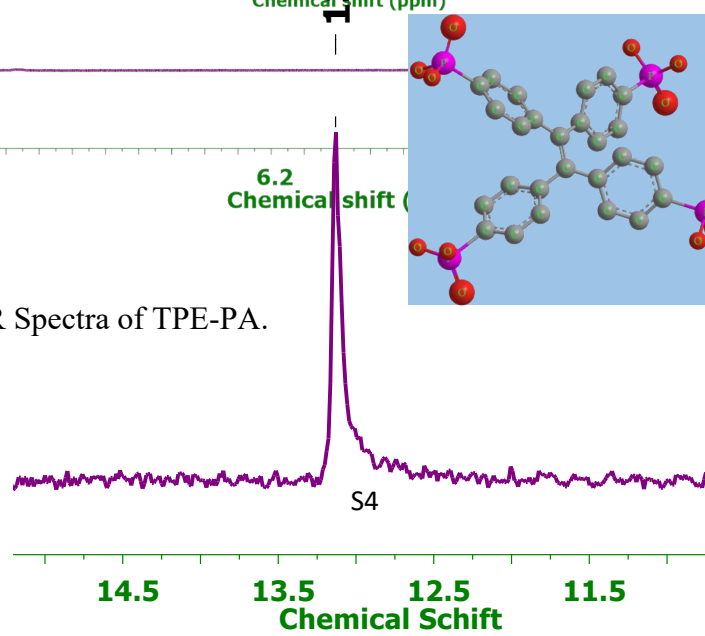


Fig. S7. ^{31}P NMR spectra of TPE-PA.

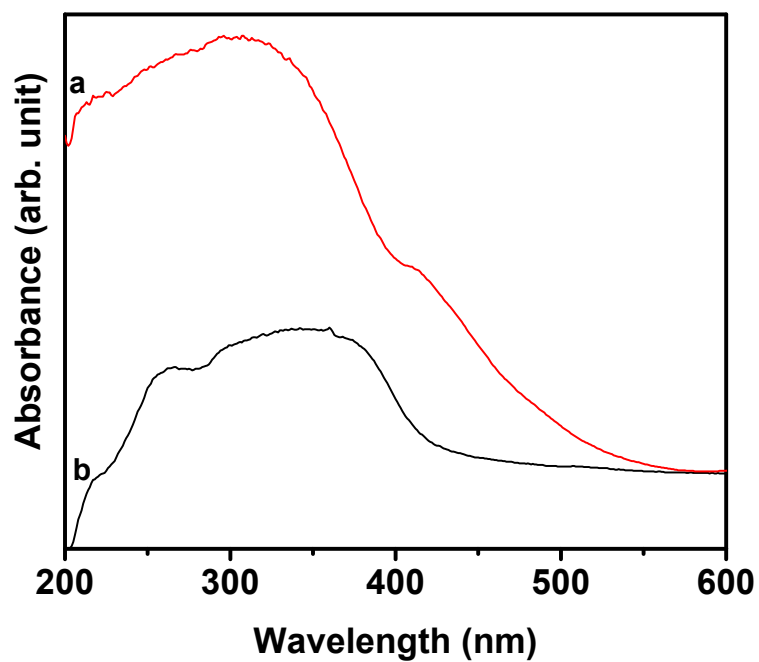


Fig. S8. Solid state UV-Visible spectra of as-synthesized H₈L-Ni-MOF (a) and H₈L-ligand (b).

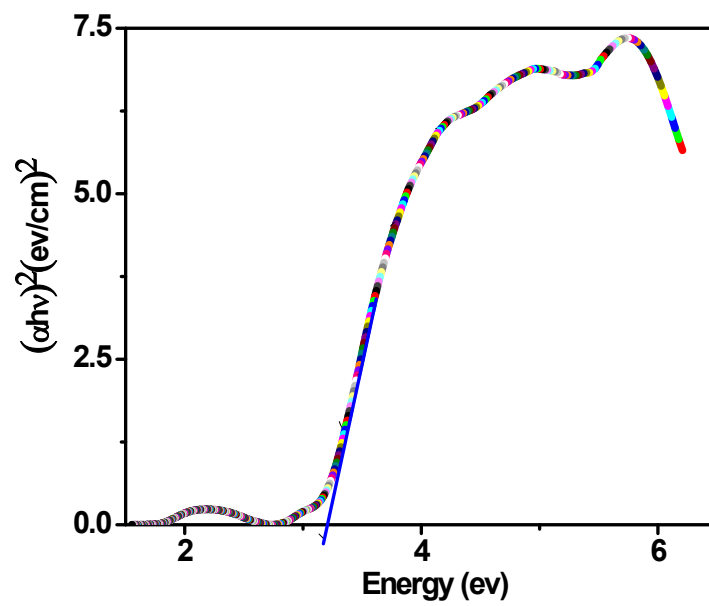


Fig. S9. Direct optical band gap of H₈L-Ni-MOF material using Tauc equation.

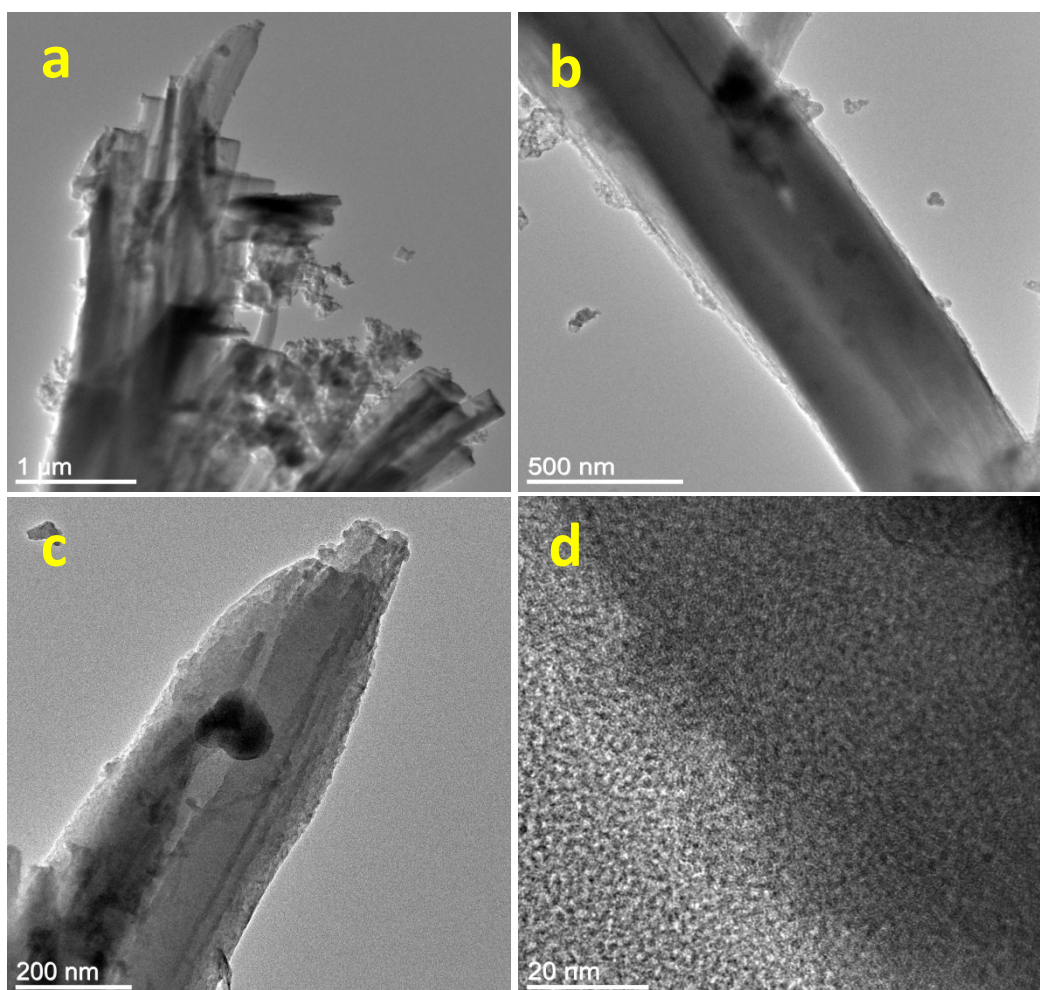


Fig. S10.UHR-TEM images with different magnification of H₈L-Ni-MOF.

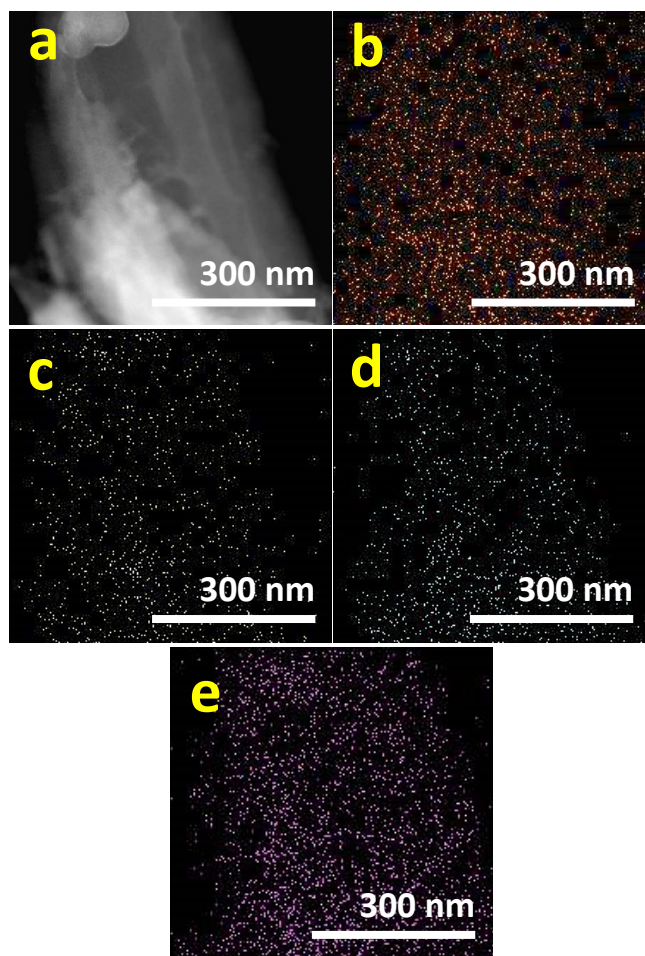


Fig. S11. HADF image and elemental mapping of H₈L-Ni-MOF material containing elements (b) C, (c) P, (d) O, and (e) Ni.

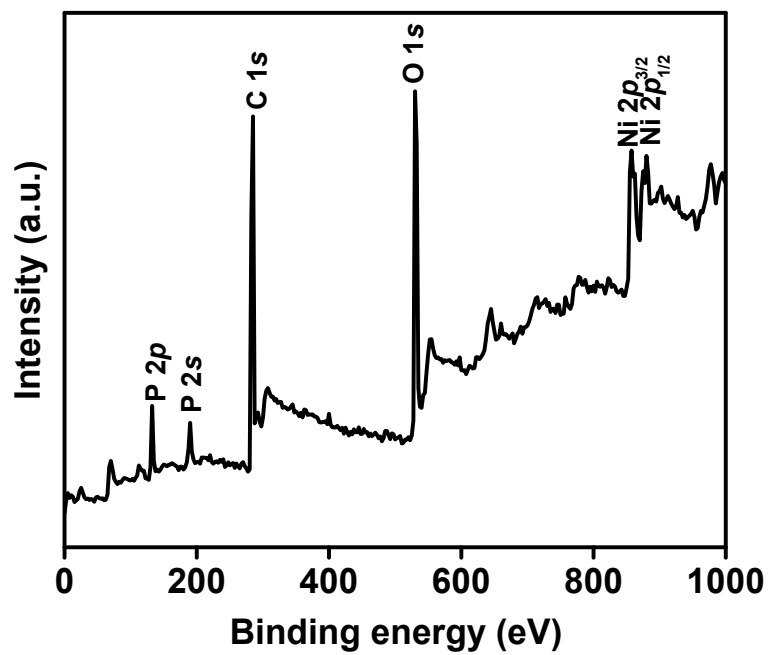


Fig. S12. Full scale XPS survey spectrum of H₈L-Ni-MOF.

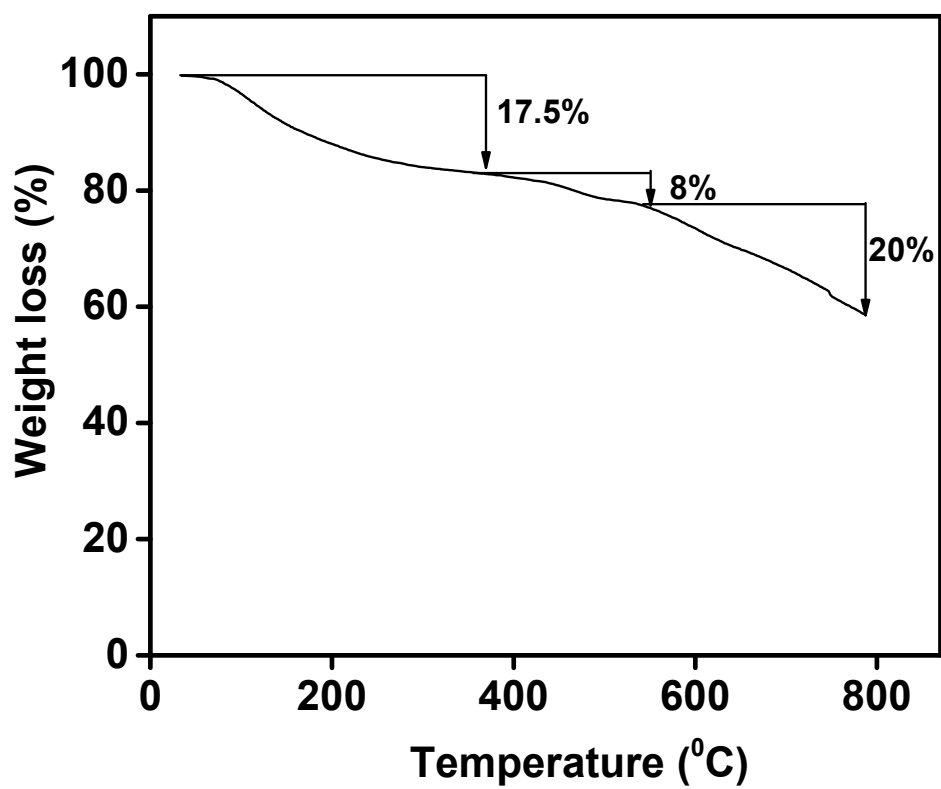


Fig. S13. TGA plot of H₈L-Ni-MOF material in N₂ atmosphere.

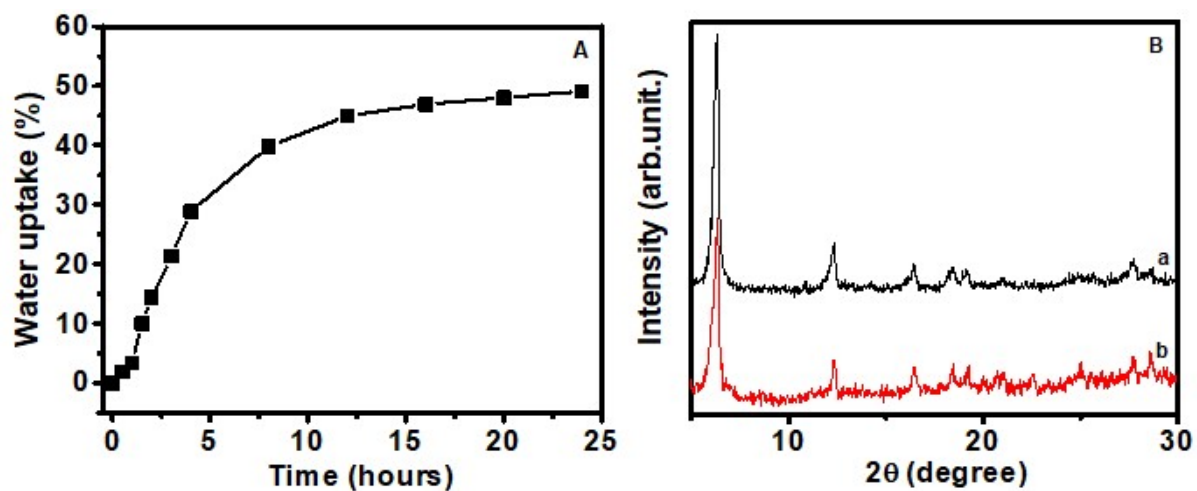


Fig. S14. Water uptake (weight %) of H₈L-Ni-MOF with time at 30 °C under 98% RH (A) and PXRD pattern of the H₈L-Ni-MOF (B) as-synthesized (a), after water uptake (b).

Table S1. Proton conductivity of H⁺@H₈L-Ni-MOF at 98% RH in different temperatures.

Temperature (°C)	Proton Conductivity (S cm ⁻¹)	
	Without doping	SA-doped sample
20	9.36×10^{-6}	3.45×10^{-3}
30	1.25×10^{-5}	4.07×10^{-3}
40	1.56×10^{-5}	4.73×10^{-3}
50	1.97×10^{-5}	5.20×10^{-3}
60	2.60×10^{-5}	6.31×10^{-3}
70	3.11×10^{-5}	7.67×10^{-3}
80	4.67×10^{-5}	9.77×10^{-3}
90	5.45×10^{-5}	1.17×10^{-2}

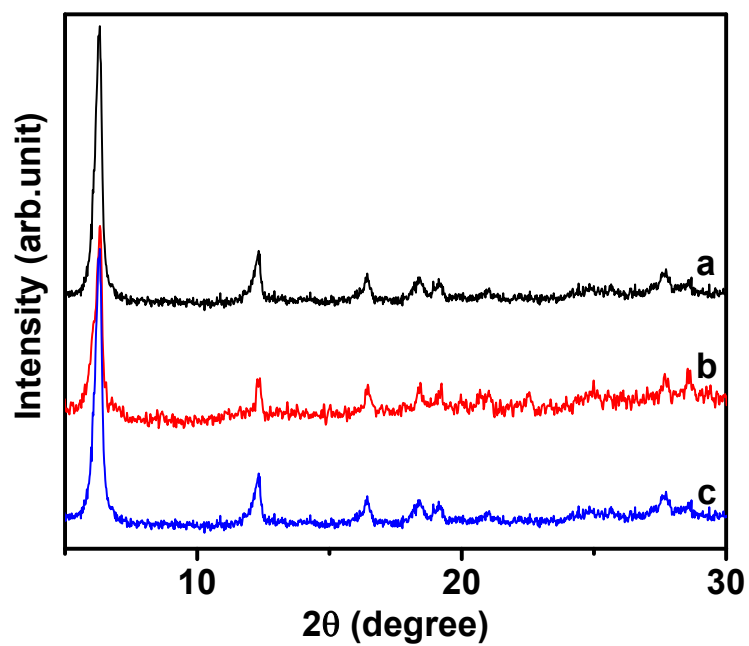


Fig. S15. PXRD pattern data of as-synthesized MOF (a), H⁺@H₈L-Ni-MOF (b), and washed H⁺@H₈L-Ni-MOF after proton conductivity measurement (c).